AGU PUBLICATIONS

Journal of Advances in Modeling Earth Systems

RESEARCH ARTICLE
10.1002/2017MS001010

Vertical Resolution Refinement in an Aqua-Planet and Its Effect on the ITCZ

M. H. Retsch[1], C. Hohenegger[1], and B. Stevens[1]

[1]Max Planck Institute for Meteorology, Hamburg, Germany

Key Points:
- Refining the vertical resolution in a General Circulation Model leads to a converging single ITCZ
- With a mean tropospheric grid spacing of 11.4 hPa a single ITCZ emerges
- Vertical discretization errors in the cumulus parameterizations lead to weak mixing and a double ITCZ for a coarse grid

Correspondence to:
M. H. Retsch,
matthias-heinz.retsch@mpimet.mpg.de

Citation:
Retsch, M. H., Hohenegger, C., & Stevens, B. (2017). Vertical resolution refinement in an aqua-planet and its effect on the ITCZ. *Journal of Advances in Modeling Earth Systems*, *9*, 2425–2436. https://doi.org/10.1002/2017MS001010

Received 7 APR 2017
Accepted 16 SEP 2017
Accepted article online 4 OCT 2017
Published online 31 OCT 2017

Abstract The General Circulation Model ECHAM is used to study the effects of three refined vertical resolutions on convection in the tropics and on the structure of the intertropical convergence zone (ITCZ). Additional vertical resolutions have 76, 134, or 192 levels, which is over four times the default resolution of 47 levels. New levels are placed in the troposphere only. The simulations are conducted on an aqua-planet with equator symmetrical, time and zonal independent sea surface temperature, and without a yearly solar cycle. Whereas the default vertical resolution shows a double ITCZ, refining the vertical resolution yields an equatorward shift of the ITCZ. The ITCZ converges to its equatorial position with 134 levels. The sensitivity of the ITCZ to the vertical resolution is traced back first and foremost to the mixing formulation in the convection scheme. Here a higher number of vertical levels leads to a stronger mixing between the updraft and its environment by design, which favors an equatorward position of the ITCZ. Differences in the relative humidity profiles explain the remaining differences in the ITCZ location. These differences can mostly be eliminated by making clouds transparent.

1. Introduction

General Circulation Models (GCMs) that have taken part in the Coupled Model Intercomparison Project phase 5 (CMIP5) discretize the vertical column with a limited number of levels, typically around 30. The Max Planck Institute Earth System Model (MPI-ESM) with its 47 vertical levels already belongs to the group of models with higher than average vertical resolution, along with EC-EARTH (62 levels) and GFDL-CM3 (48 levels). Differences in the total number of vertical levels do not necessarily reflect the free troposphere resolution, taken here as the region between 900 and 250 hPa, as they often reflect differences in the resolution of the boundary layer and/or choices of model top. Except for EC-EARTH, CMIP5 models employ between 8 and 16 levels to discretize the free troposphere with a median of 12 levels. This gives a typical grid spacing of about 55 hPa or 750 m. To put these numbers into context, consider that the scale height of water vapor in the atmosphere is only 2 km. Hence to resolve moisture variations a much finer resolution is required. Tompkins and Emanuel (2000) concluded that a vertical resolution of 25 hPa is needed to correctly capture the vertical distribution of water vapor in radiative convective equilibrium. From a different perspective, consider that dry intrusions in the tropics may not be much thicker than 1 km (see Figure 2 from Redelsperger et al. (2002)). Dry intrusions are thought to play an important role in the regulation of the tropical climate, not only through their very distinct radiative properties (e.g., Mapes & Zuidema, 1996) but also by suppressing deep convection in favor of cumulus congestus clouds (e.g., Jensen & Genio, 2006; Takemi et al., 2004). In fact, an inaccurate representation of the sensitivity of the convection scheme to ambient relative humidity (Derbyshire et al., 2004) has often been invoked as a cause for major precipitation biases in the tropics including the double ITCZ problem (e.g., Möbis & Stevens, 2012; Oueslati & Bellon, 2013), distorted MJO (e.g., Kim et al., 2014; Slingo et al., 2002) or too weak convective activity under monsoon conditions (Roca et al., 2005).

The position of the ITCZ has been a long-lasting problem in climate simulations, with GCMs exhibiting a double ITCZ structure that is not evident in observations (e.g., Li & Xie, 2014; Lin, 2007; Mechoso et al., 1995). Even when using prescribed sea surface temperatures, two parallel bands of rain that straddle the equator are apparent in many models (Medeiros et al., 2015). For such models, the design of the convection scheme is believed to be one of the root causes of the double ITCZ problem (e.g., Bacmeister et al., 2006; Möbis & Stevens, 2012; Oueslati & Bellon, 2013; Zhang & Mu, 2005). Even in aqua-planets, modifying the

representation of convection can lead to various ITCZ locations, from a single ITCZ located at the equator to various off-equatorial positions (e.g., Möbis & Stevens, 2012). Cloud radiative effects are another factor that has been shown to affect the position of the ITCZ (Crueger & Stevens, 2015; Harrop & Hartmann, 2016). Although not directly tested in the aforementioned studies, both cloud radiative effects and the behavior of the convection scheme are dependent upon the chosen underlying vertical resolution so that a sensitivity of the position of the ITCZ to the vertical resolution is likely possible. Williamson (2013) explicitly tested such a sensitivity. He conducted aqua-planet simulations with the CAM3 models employing 26, 30, and 60 vertical levels. The simulations converged with more levels to a double ITCZ structure with an ITCZ located around 3.5° (see his Figure 3). The cause for this behavior was traced back to unrealistically large amount of low clouds in the planetary boundary layer of the high resolution runs due to missing ventilation by the shallow convection scheme that became inactive with enhanced vertical resolution. Besides a potential sensitivity to the vertical grid spacing, the ITCZ structure has also be shown to depend upon the horizontal resolution in aqua-planet simulations (Landu et al., 2014).

The goal of this study is to assess the sensitivity of the ITCZ location to the vertical resolution and to trace back this sensitivity to specific dependencies of the employed parameterizations on the vertical grid spacing. As a side goal, the convergence of the simulations is assessed. To pursue our goals, an aqua-planet setup is used and the number of vertical levels is refined, from 47 to 76, 134, and finally 192 levels. This gives a vertical resolution of maximum 7.6 hPa in the free troposphere, well below the 25 hPa threshold of Tompkins and Emanuel (2000). Our study is akin to the study of Williamson (2013) with the major differences that we span a greater range in vertical resolution and use another GCM and, in particular, another convection scheme. Our shallow convection scheme does not shut down when the vertical resolution is refined and, as will be shown, the simulations converge toward one single ITCZ. Also older studies that have documented the sensitivity of different aspects of the tropical climate to the vertical resolution (e.g., Inness et al., 2001; Pope et al., 2001; Roeckner et al., 2006) have considered vertical resolutions similar to the ones now in use in the CMIP5 models, which is relatively coarse.

The outline of the study is as follows. Section 2 briefly describes the model used and the experimental setup. The sensitivity of the ITCZ position to the vertical resolution is documented in section 3. Section 4 then presents results of additional sensitivity experiments where the dependency of the ITCZ on the vertical resolution is successively removed. The findings are summarized in section 5.

2. Method

2.1. Model

The General Circulation Model ECHAM version 6.3.1, which is the atmosphere component of the MPI-ESM, is used (denoted ECHAM hereafter). A description of the dry adiabatic core and of the diabatic processes is given in Stevens et al. (2013). In comparison to the version used in Stevens et al. (2013), ECHAM 6.0, updates include bug fixes, in particular in the computation of the subgrid cloud cover. The latter could erroneously only take values of 0 and 1 in the previous version, leading to blinking clouds and a weaker cloud cover. These updates led to a change in the ITCZ structure, likely due to changes in cloud radiative effects as found in other studies (Harrop & Hartmann, 2016; Möbis, 2013). The ITCZ now exhibits a double precipitation peak in the tropics (see section 3), in contrast to Möbis and Stevens (2012) who obtained a single ITCZ when using ECHAM 6.0. The convection scheme itself has remained unchanged though. Given their importance for this study, some of the key characteristics of the convection scheme as well as of the cloud cover scheme are highlighted in the following. A detailed description of the convection scheme can be found in Möbis and Stevens (2012).

ECHAM employs a convection scheme based on Tiedtke (1989) and modified by Nordeng (1994) in which three types of convection are possible: shallow, midlevel, and deep. The convection scheme is a bulk mass flux scheme. It consists of one up downdraft and one downdraft, which entrain and detrain air through "turbulent" and "organized" mixing processes. In the updraft turbulent mixing accounts for subgrid scale mixing at cloud edges and is parameterized by using constant entrainment (which is set to zero under some circumstances) and detrainment rates. Organized mixing accounts for large-scale organized inflow at cloud base and outflow at cloud top. Its mixing rates are dependent upon the updraft's properties, in particular buoyancy.

The closure of deep convection is based on convective available potential energy (CAPE) that is consumed over a given decay time scale. For shallow convection, a closure based on moisture convergence is used.

The cloud cover scheme uses the approach of Sundqvist et al. (1989) based on a relative humidity threshold to parameterize fractional cloud cover. The condensation threshold is a function of height and should theoretically be reconsidered when changing resolution (see Xu & Krueger, 1991). In this study, the threshold nevertheless remained the same in all experiments to not mask any resolution dependency. The resulting cloud cover C is computed as $1-\sqrt{1-\frac{r-r_0}{r_s-r_0}}$, where r is the relative humidity, r_s is the saturation value (which is 1), and r_0 is the relative humidity threshold.

2.2. Experimental Setup

ECHAM is run with a horizontal spectral truncation of T63 and as an aqua-planet in all conducted experiments. The aqua-planet setup follows Neale and Hoskins (2000). Hence, neither landmasses nor sea ice exist in the model. There are also no seasonal variations and equinox conditions as of 21 March are imposed throughout the year. Sea surface temperature (SST) is prescribed and zonally symmetrically distributed. The "Qobs" distribution of Neale and Hoskins (2000), which most closely resembles the observations, is used. SST is calculated for latitudes φ as

$$\mathrm{SST}(\varphi)=\begin{cases} T_{\max}\cdot\left(1-\frac{1}{2}\sin^2\left(\frac{3\varphi}{2}\right)-\frac{1}{2}\sin^4\left(\frac{3\varphi}{2}\right)\right) & : \quad |\varphi|<\frac{\pi}{3} \\ 0^\circ\,\mathrm{C} & : \quad \text{else} \end{cases} \tag{1}$$

where SST is the sea surface temperature in °C and $T_{\max}$ is the maximum temperature at the equator, which equals 27°C in Qobs.

The vertical coordinate in ECHAM is based on hybrid σ-levels, i.e., the pressure value for each "full" level p_i is computed as the average of two neighboring "half" levels $\hat{p}$, one above the full level and one below it. The pressure of a half level depends on two parameters a and b and the surface pressure $\hat{p}_0$:

$$\hat{p}_i=a_i+b_i\cdot\hat{p}_0 \tag{2}$$

$$p_i=(\hat{p}_i+\hat{p}_{i+1})/2 \tag{3}$$

The standard ECHAM configuration employs 47 full levels and is called L47. This serves as a control simulation. From this vertical distribution, three new level setups with decreased vertical spacing between levels are created. For a given surface pressure $\hat{p}_0$ of 1,000 hPa, the default L47 and the new main level distributions are shown in Figure 1. The new distributions feature 76, 134, and 192 main levels and thus are called L76, L134, and L192. L76 is calculated by adding one half level between each pair of the L47 half levels:

$$\hat{p}_i^{76}=\begin{cases} \hat{p}^{47}_{(i-19)/2+19} & : \quad i \text{ is odd} \\ \frac{1}{2}\left(\hat{p}^{47}_{\lceil(i-19)/2\rceil+19}+\hat{p}^{47}_{\lfloor(i-19)/2\rfloor+19}\right) & : \quad i \text{ is even} \end{cases} \tag{4}$$

where $\hat{p}^{76}$ denotes half level pressures of the 76 levels grid, $\hat{p}^{47}$ denotes half level pressures for the default grid and $i\in[20,77]$. Resolution refinement is confined to the troposphere only, so additional levels are introduced solely below a pressure of 50 hPa. L134 is calculated in a similar way, but with one new half level added between each pair of the L76 half levels. Finally L192 is based upon L76 as well. But now we place two new L192 half levels in equidistance between each pair of the L76 half levels. The resulting maximum vertical spacing in the troposphere between half levels amounts to 45.6 hPa in L47, 22.8 hPa in L76, 11.4 hPa in L134, and 7.6 hPa in L192.

Due to the refinement of the vertical grid spacing the time step had to be adapted in some experiments. The time step for L47 and L76 is 450 s. For L134 it is 240 s, whereas it is shortened to 150 s for L192. Repeating the L47 experiment with a time step of 150 s had no effect on the structure of the ITCZ (not shown).

All experiments are run over an integration time period of 5 years, allowing for a spin up phase of 2 and 3 years of sampling data. Following Möbis and Stevens (2012) as well as Medeiros et al. (2008), this is sufficient given that internal variability longer than 3 years is of negligible importance. All figures presented in

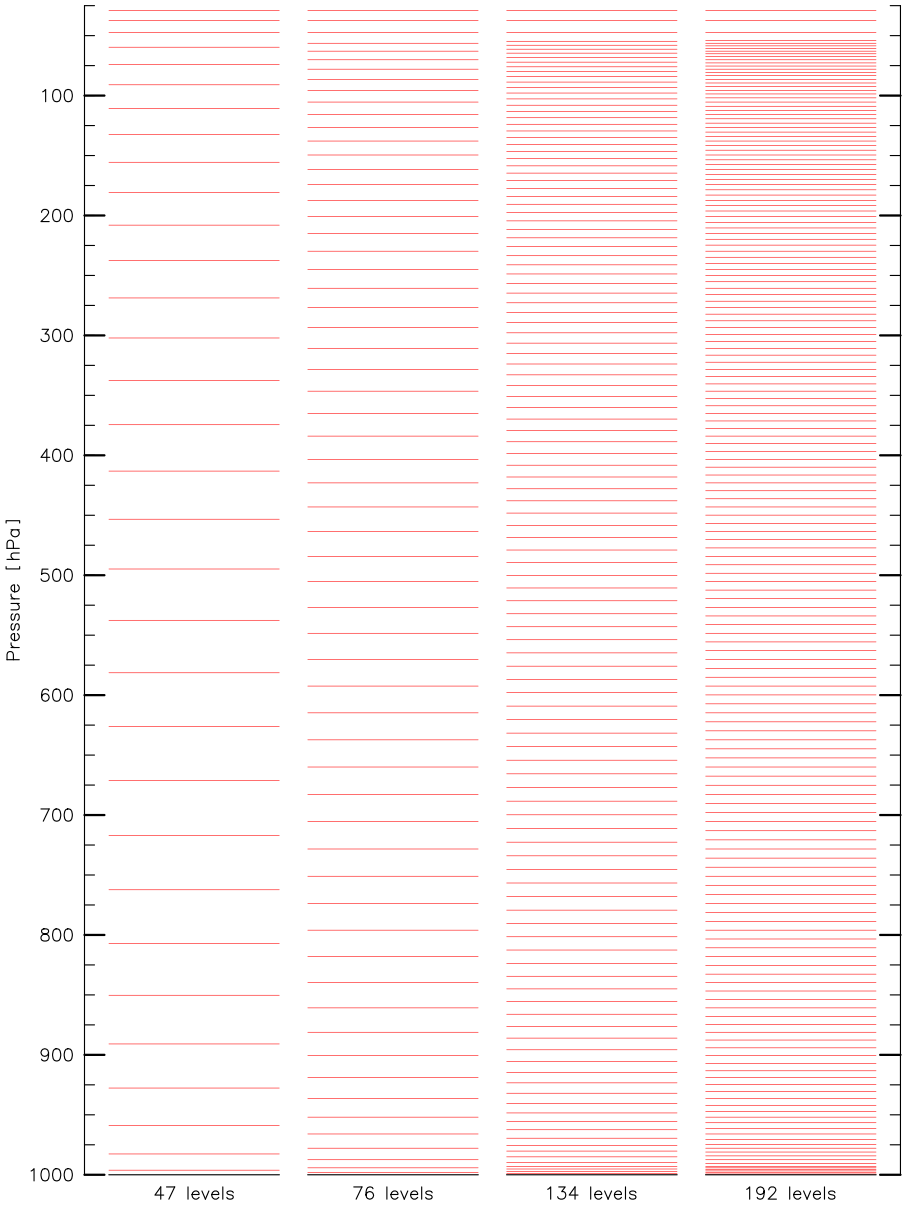

Figure 1. Distribution of model full levels for the various experiments. The *y* axis ends at 25 hPa.

this study represent averages over these last 3 years and are averaged in the zonal direction unless noted otherwise.

3. Time-Zonal Average Effects of Vertical Resolution

Figure 2 shows the latitudinal precipitation distribution for the set of experiments, focusing on the tropical region. There is a clear trend toward a single ITCZ structure when decreasing the vertical grid spacing (see Table 1 as well for a summary of the ITCZ location in the various experiments). The ITCZ, defined here as the latitude of maximum precipitation, is located at the grid point center of |8.4°| in L47, moves closer to the equator in L76 with a mean location at |4.7°|, and collapses to a single ITCZ structure located at the equator in L134 and L192. The single ITCZ structure is established in L134 and does not change significantly with a further reduction of the grid spacing. Therefore, the model converges to the solution of a single ITCZ, which is akin to what is observed over the Pacific (Li & Xie, 2014; Lin, 2007). A switch from a double to a single ITCZ was obtained in the aqua-planet simulations of Möbis and Stevens (2012), albeit when switching

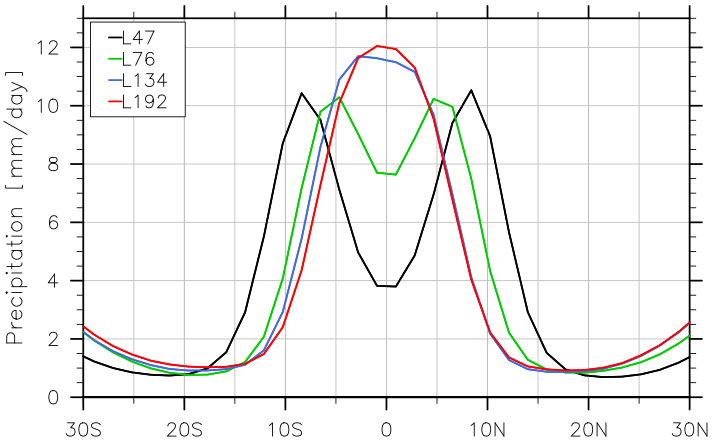

Figure 2. Total precipitation for L47, L76, L134, and L192 experiments.

from the Tiedtke to the Nordeng convection scheme. In their study, the ITCZ shifted by 7°. Hence, changing the vertical resolution has actually a stronger effect on the location of the ITCZ than changing convection schemes in ECHAM.

The transition from a double to a single ITCZ (Figure 2) is accompanied by an increase of precipitation at the equator and a decrease of precipitation at the latitude of the former maxima. It is nevertheless not related to a change in precipitation type. In all the simulations, convective precipitation dominates. The ratio between convective and large-scale precipitation amounts to at least 80% equatorward of |10°| for all conducted experiments and does not change significantly with vertical resolution. Also the global mean precipitation only slightly varies with resolution with values of 3.17 mm/d in L47, 3.32 mm/d in L76, 3.33 mm/d in L134, and 3.30 mm/d in L192.

The transition of the ITCZ structure toward a single ITCZ is further mirrored in cloud cover, cloud ice content, and relative humidity (not shown), which, given their link to convection, is not surprising. The cloud water content though (see Figure 3) exhibits a more interesting behavior. The maxima in cloud water content between 900 and 800 hPa increases with decreasing vertical grid spacing, at least up to L134. More importantly a secondary maximum in cloud water content appears at 600 hPa, between −5° and 5°, as the grid spacing is reduced. It is strongest in L192. As all the experiments are dominated by convective precipitation, the main source of cloud water content is hypothesized to be detrained water from the convection scheme. The increase of cloud water content could indicate an increase of the parameterized bulk convective plumes terminating at this height, reminiscent of a cumulus congestus mode (Johnson et al., 1999). Comparing simulations using 30 and 19 vertical levels, Inness et al. (2001) found an increase of convective clouds terminating around 600–500 hPa that they associated with the development of more stable layers in their vertically refined simulations. The development of such layers resulted from the melting of ice that, for the same amount of heat, leads to stronger cooling in thinner layers.

Figure 4 correspondingly shows a histogram of the height at which convection terminates, as obtained from the convection scheme, from all three convection types and for each experiment with a bin width of 20 hPa. A clear higher frequency of convective plumes terminating around 600 hPa between −5° and 5° as the vertical grid spacing is refined is not supported. Instead 14% less plumes are terminating in L192 compared to L47 between 500 and 700 hPa at the equator. At the respective latitudes of peak precipitation, given in Table 1, a similar amount of plumes are terminating across the simulations with a standard deviation of 8.7%. The rather discretely distributed convective tops between 700 and 500 hPa in L47 appear more concentrated around 600 hPa in the other experiments. The cloud top heights of deep convection, i.e., cloud tops at a height of 200 hPa and above, also only exhibit a weak sensitivity upon the chosen vertical grid spacing with a tendency to reach slightly higher levels with finer vertical resolution.

Alternatively, the secondary maximum in cloud water content of Figure 3 may just indicate a change in detrained water while the convective clouds rise through the atmosphere. Integrating the cloud water content between 700 and 500 hPa and averaging it between −5° and 5°, the amount of cloud water is

Table 1
Averaged Latitude of Precipitation Maximum for Various Model Experiments

Levels	Model configuration Standard	No mixing	Clouds-off	No mixing and clouds-off
47	8.4°	12.1°	10.3°	12.1°
76	4.7°	12.1°	8.4°	12.1°
134	Equator	10.3°	6.5°	12.1°
192	Equator	8.4°	4.7°	12.1°

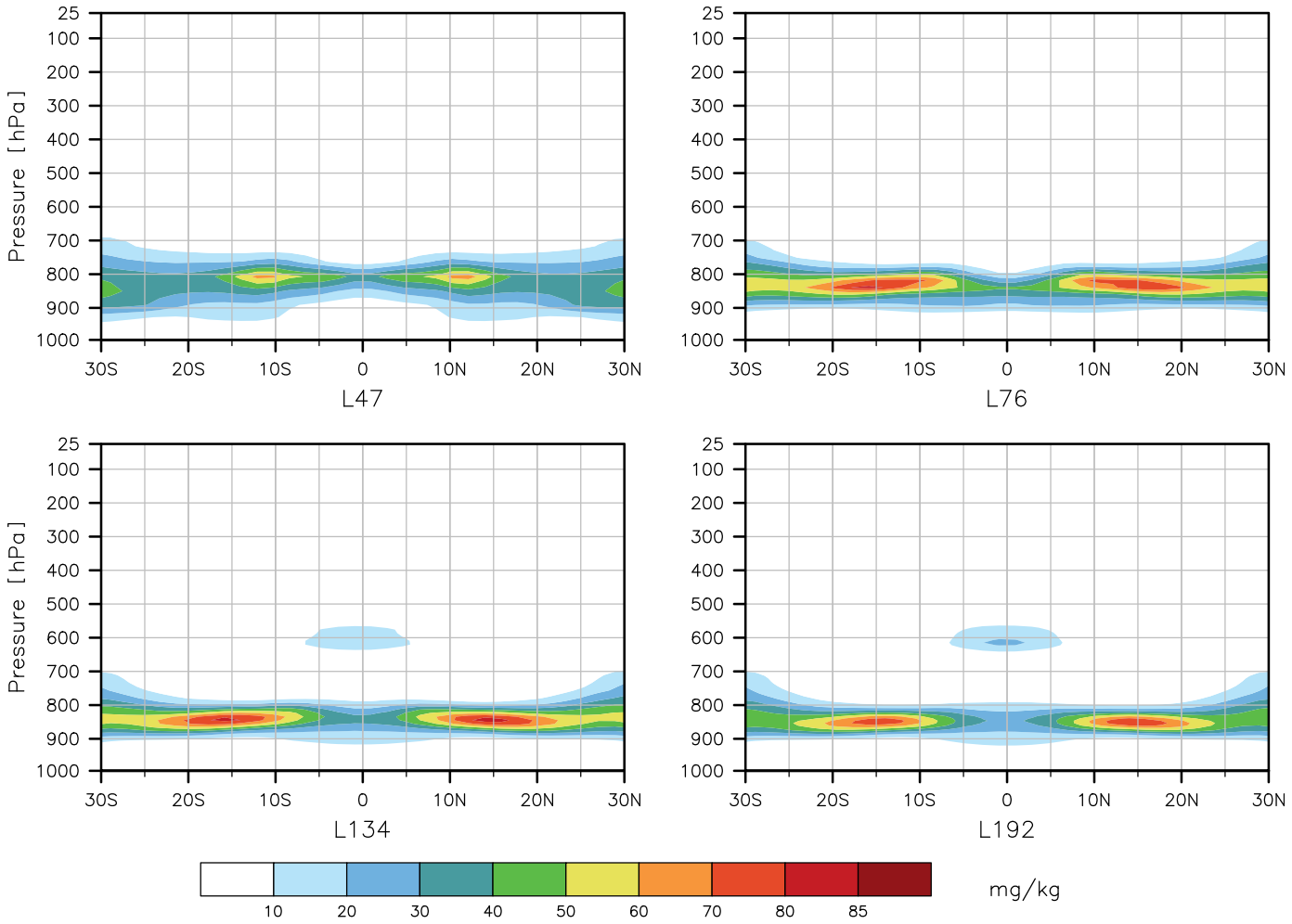

Figure 3. Cloud water content for L47, L76, L134, and L192 experiments.

0.0018 mm in L47, 0.0055 mm in L76, 0.013 mm in L134, and 0.015 mm in L192. This indicates that the secondary maximum in cloud water content is not a mere consequence of the thinning of the vertical layer given the same amount of detrained water but that, as the vertical grid spacing is refined, more water is actually detrained. More detrained water from the convection scheme hints at stronger mixing and/or at a stronger sensitivity of the convection scheme to ambient atmospheric conditions. Suppressing deep convective clouds in drier atmospheric conditions through the use of larger entrainment rates and hence stronger mixing has been found to be beneficial in past studies for maintaining a single ITCZ at the equator (Möbis & Stevens, 2012; Oueslati & Bellon, 2013). This fits our results, a hypothesis that is further investigated in the next section.

4. Sensitivity Experiments to Explain the Dependency on Vertical Resolution

4.1. Turning Off Updraft Mixing

In the previous section, it has been hypothesized that a dependency of the convective mixing process upon the vertical grid spacing exists and explains the change in ITZC structure.

Depending on the decrease or increase of mass flux with height, reduced grid spacing leads to decreased or increased mixing, respectively. If more environmental air is mixed, the updraft loses more of its buoyancy due to the evaporative cooling associated with the mixing of dry environmental air into the updraft. The updraft does not experience as much upward propulsion. Eventually the buoyancy respective to the

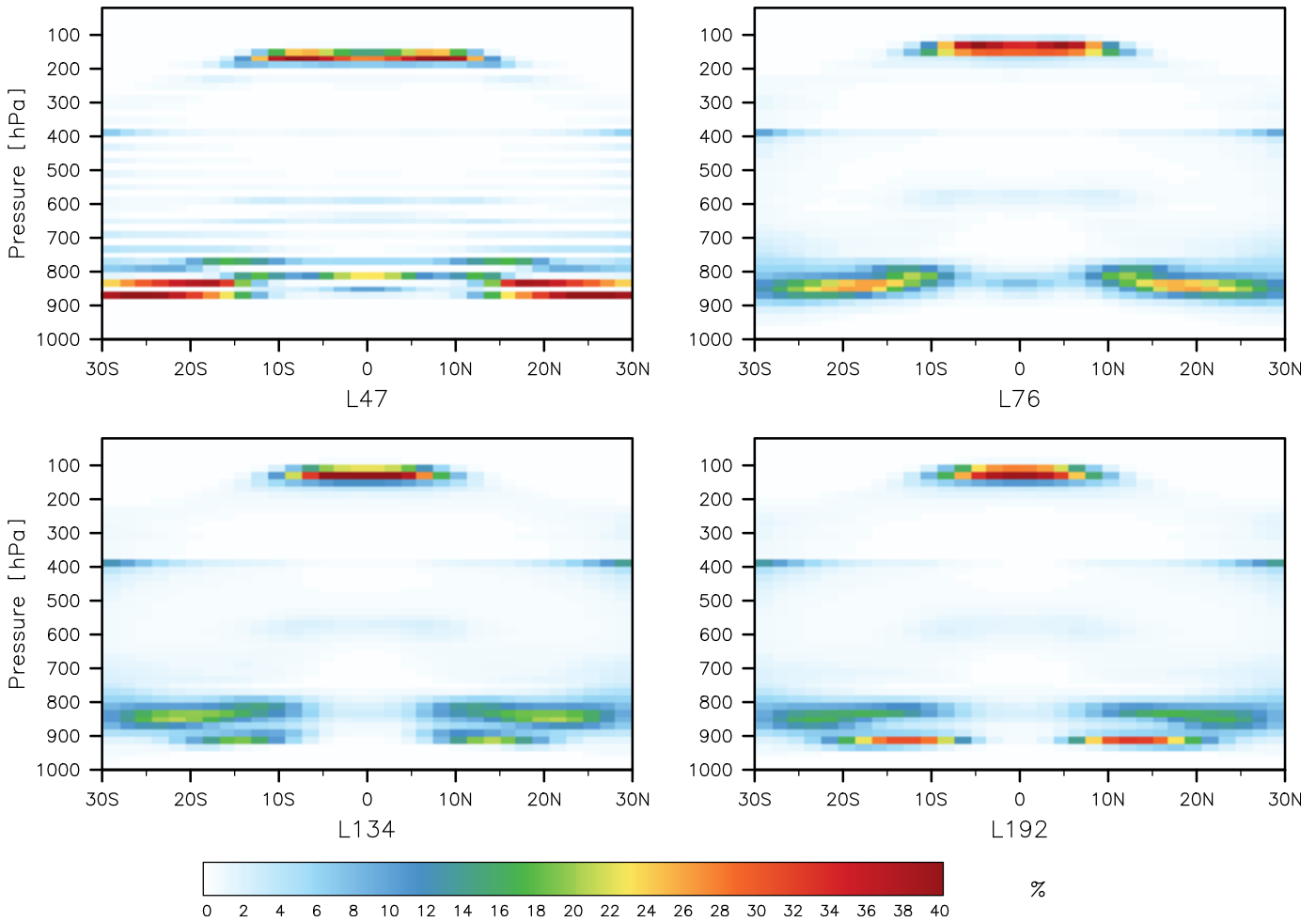

Figure 4. Histogram of convective cloud tops as obtained in the convection scheme for L47, L76, L134, and L192 experiments. Probability equals 100% for all heights per latitude.

environment is zero and convection terminates. As the poleward flank of the ITCZ tends to be drier than the equatorward flank, a convection scheme that is more sensitive to mixing with dry air will move equatorward, where the convection is less penalized.

The updraft equations read:

$$\frac{\partial M}{\partial z} = E_{\mathrm{trb}} - D_{\mathrm{trb}} + E_{\mathrm{org}} - D_{\mathrm{org}} = \varepsilon M - \delta M + E_{\mathrm{org}} - D_{\mathrm{org}} \tag{5}$$

where M is the updraft mass flux, E_{trb} and D_{trb} are the turbulent entrainment and detrainment, E_{org} and D_{org} are the organized entrainment and detrainment. E_{org} and D_{org} are related to the updraft buoyancy, whereas the turbulent terms are assumed to be proportional to the mass flux with fixed values for ε and δ. The organized entrainment term is calculated as:

$$E_{\mathrm{org}} = M\left(\frac{b}{2}\left(w_{\mathrm{cb}}^2 + B\right)^{-1} + \frac{1}{\rho}\frac{\mathrm{d}\rho}{\mathrm{d}z}\right) \tag{6}$$

with the buoyancy b at height z, w_{cb} is the cloud base vertical velocity, B is the vertically integrated buoyancy of the parameterized updraft from cloud base until the height z, and ρ is the density. For the organized detrainment, it is:

$$D_{\text{org}} = M \frac{1}{\sigma} \frac{\partial \sigma}{\partial z} \quad \text{with} \quad \sigma = \sigma_0 \cos\left(\frac{\pi}{2} \frac{z - z_{\text{low}}}{z_{\text{ct}} - z_{\text{low}}}\right) \tag{7}$$

and σ is the horizontal area covered by the updraft, z_{ct} is the parameterized bulk cloud top height, and z_{low} is the lowest possible organized detrainment height. A more detailed description of equations (5)–(7) is presented in Möbis and Stevens (2012). The updraft equations are discretized using a simple first-order scheme. Considering only turbulent entrainment, equation (5) is discretized in ECHAM as follows:

$$M^{(k-1)} = M^{(k)} + \varepsilon M^{(k)} \cdot \Delta z^{(k-1)} \tag{8}$$

$$M^{(k-2)} = M^{(k-1)} + \varepsilon M^{(k-1)} \cdot \Delta z^{(k-2)} \tag{9}$$

$$= M^{(k)} + \varepsilon M^{(k)} \cdot \Delta z^{(k-1)} + \varepsilon M^{(k)} \cdot \Delta z^{(k-2)} + \varepsilon^2 M^{(k)} \cdot \Delta z^{(k-1)} \Delta z^{(k-2)} \tag{10}$$

$$\neq M^{(k)} + \varepsilon M^{(k)} \cdot \left(\Delta z^{(k-1)} + \Delta z^{(k-2)}\right) \tag{11}$$

with level numbers increasing toward the surface and $\Delta z^{(k-1)}$ as the height difference between level k and $k-1$. Putting all the terms together in equation (10) gives a supplementary entrainment of $\varepsilon^2 M^{(k)} \cdot \Delta z^{(k-1)} \Delta z^{(k-2)}$ when having an additional level $k-1$ between k and $k-2$. Without the level $k-1$, the mass flux at level $k-2$ would be computed according to equation (11). The scheme is first order in its convergence properties, which requires a rather fine discretization to make truncation errors small. The integral will converge for small enough values of Δz, which may explain the converging behavior seen in section 3. Likewise, considering only turbulent detrainment, a supplementary detrainment of $\delta^2 M^k \cdot \Delta z^{(k-1)} \Delta z^{(k-2)}$ would occur, consistent with the larger amount of detrained water observed in section 3 with decreased Δz. The employed discretization will also lead to slightly distinct and additional terms for the organized entrainment and organized detrainment.

To test the idea of enhanced mixing, the previous experiments are repeated with ε, δ and D_{org} set to zero. The sensitivity of the ITCZ does not depend on D_{org} for the experiments where only the mixing is removed, i.e., the same ITCZ structures would emerge when only setting ε and δ to zero. But in the experiments of section 4.2, where also cloud radiative effects are removed, a sensitivity of the ITCZ location upon the vertical grid spacing remains if D_{org} is not removed. This indicates that D_{org} weakly depends upon the grid spacing. As can be seen by comparing equations (5) and (7), the Δz-term cancels, which is not the case for the turbulent detrainment. In contrast, additionally setting E_{org} to zero does not further alter the sensitivity of the ITCZ location to the vertical grid spacing. This is related to the fact that only close to plume base the organized entrainment contribution is larger than the turbulent one, whereas the sensitivity to the grid spacing seems to manifest itself in the middle troposphere (see Figures 3 and 4). The experiments are called "NM47," "NM76," "NM134," and "NM192," where NM stands for "No Mixing." The differences in the location of the ITCZ across the different vertical resolutions (Figure 5) have become much smaller. NM134 and NM192 shift their precipitation maximum by only 2° and 4°, respectively, toward the equator compared to NM47, against 8° when mixing is allowed (see Table 1). Compared to their counterpart experiments of Figure 2 all the new experiments exhibit a double ITCZ with a more poleward location. Reducing mixing shifts the ITCZ poleward, which is consistent with the results of Möbis and Stevens (2012) and Oueslati and Bellon (2013) who investigated the dependency of the ITCZ position upon entrainment rate. Hence, Figure 5 supports the hypothesis that enhanced mixing with smaller Δz is the primary cause for the transition from a double to a single ITCZ.

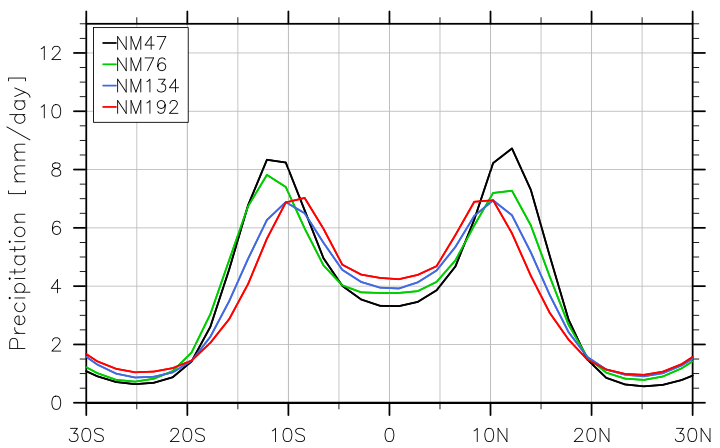

Figure 5. Total precipitation for NM47, NM76, NM134, and NM192 experiments without mixing.

A simple solution to this problem could be to correct the entrainment rate to mimic a stronger mixing as obtained at finer resolution. This can be done by adding a term $\varepsilon^2 M^{(k)} \cdot \Delta z^{(k-1)} \Delta z^{(k-2)}$ and $\delta^2 M^{(k)} \cdot \Delta z^{(k-1)} \Delta z^{(k-2)}$ to the updraft equation of the L47 version. Applying the equivalent terms of L134 to the computation of deep convection in L47 indeed led to a shift of the ITCZ, now located at 1.85° versus 8.4° in L47 and equatorial in L134. The peak

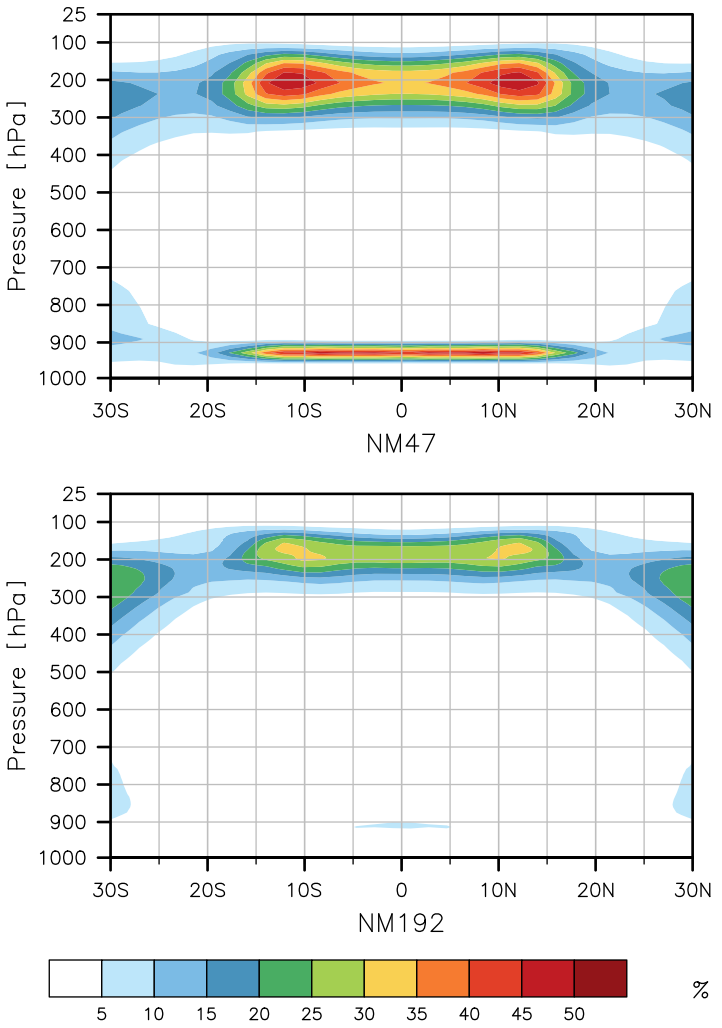

Figure 6. Cloud cover for NM47 and NM192 experiments.

precipitation amount also increased from 10.5 to 11 mm/d, in better agreement with L134 (11.7 mm/d).

Differences that remain between the NM experiments are indicative of differences that cannot be explained by the errors from the low-order solutions to the updraft equation (equation (5)). These are especially marked in the cloud cover distribution. This is shown in Figure 6 using the two extreme resolutions. NM192 exhibits up to 45% less cloud cover than NM47, both at a height of 950 and 200 hPa. A strong increase is also found in the cloud water content around 950 hPa in NM47 compared to NM192 (not shown).

In principle, cloud radiative effects are expected to lead to a contraction of the ITCZ (Crueger & Stevens, 2015; Harrop & Hartmann, 2016; Möbis, 2013). Applying this argument to the results of NM47 and NM192, a more equatorward position of the ITCZ would be expected in NM47, opposite to what is obtained in Figure 5. Möbis (2013) nevertheless showed that the position of clouds in the vertical column affects the response of the ITCZ location to cloud radiative effects. Low-level clouds, in contrast to high clouds, yield a poleward shift of the ITCZ. Hence, the much stronger low-level cloud radiative effect in NM47 compared to NM192 can partly explain the more poleward location of the ITCZ in NM47. Making clouds transparent to the radiation below 700 hPa in NM47 (not shown) indeed shifts its ITCZ equatorward by circa 1.8°.

4.2. Clouds Made Transparent

Given the previous discussion, it is clear that cloud radiative effects affect the position of the ITCZ. They may do so indirectly, by amplifying the effects of remaining humidity differences between the simulations, or directly, through a dependency of the cloud cover scheme on the vertical resolution. These issues are examined in this section.

Experiments in which clouds are made transparent to radiation, "CO47," "CO76," "CO134," and "CO192," with CO for "Clouds-Off," are first conducted to assess the strongest potential impact of cloud radiative effects on the ITCZ location. Making clouds transparent to radiation was proposed and used in Randall et al. (1989) and also in COOKIE (Clouds On/Off Klimate Interaction Experiment, Crueger & Stevens, 2015) to study the radiative effects of clouds on circulations. As shown in Figure 7, the ITCZ exhibits a double structure in all four experiments with Clouds-Off, with a more poleward location than in the corresponding standard experiments. This is consistent with the results of Möbis (2013), Crueger and Stevens (2015), and Harrop and Hartmann (2016). More importantly, the spread in the location of the ITCZ among the experiments is reduced with a maximum difference of 5.6° between CO47 and CO192 versus 8.4° between L47 and L192 (see Table 1). The effect is nevertheless weaker than the one associated with the representation of mixing processes, indicating that cloud radiative effects are at best a secondary cause to the spread in ITCZ location with vertical grid spacing.

That the ITCZ structure in CO47 and CO192 remains distinct is not too surprising given their different representation of mixing processes and hence distinct relative humidity profiles. As a second step, the model is thus run in each vertical configuration with no mixing of the updraft with the environment and no cloud radiative effect. Total precipitation for "NMCO47," "NMCO76," "NMCO134," and "NMCO192" experiments (NMCO for "No Mixing and Clouds-Off") is shown in Figure 8. The spread in the ITCZ location almost vanishes (see also Table 1). The difference of the ITCZ structures in terms of precipitation amount also decreases substantially, with only up to 0.5 mm/d difference in between 10°S and 10°N.

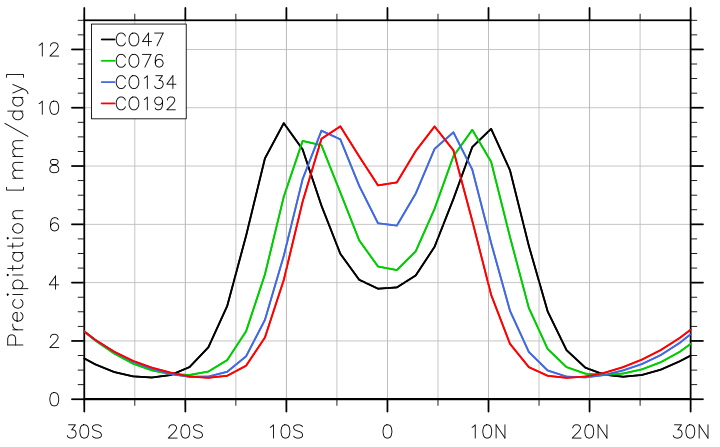

Figure 7. Total precipitation for CO47, CO76, CO134, and CO192 experiments without clouds.

The question remains as to whether the sensitivity of the ITCZ structure to cloud radiative effects results from a sensitivity of the cloud cover parameterization to the vertical grid spacing, e.g., due to an inadequate formulation of the critical relative humidity threshold, or from different relative humidity profiles passed to the cloud cover parameterization. Figure 9 shows the cloud cover and relative humidity distributions for the two extreme cases: NMCO47 and NMCO192. Cloud cover differences seem to reflect corresponding differences in the relative humidity distribution. NMCO47 is moister than NMCO192 above 300 hPa and below 900 hPa, which is consistent with the larger cloud cover of NMCO47 above 300 hPa and below 900 hPa. Further differences in relative humidity can be noticed between 900 and 300 hPa but they do not lead to changes in cloud cover. Degrading the high-resolution relative humidity profile to low resolution and applying the cloud cover scheme (see end of section 2.1) as a diagnostic tool also confirms that the sensitivity of the ITCZ structure almost exclusively results from differences in the relative humidity profile and not from the cloud cover parameterization per se. The obtained cloud cover profiles remain similar in that case. This means that other processes in the convection scheme, like the trigger function or the fact that the mass flux that overshoots is simply detrained in one grid box, lead to differences in the relative humidity profile among the simulations and the cloud cover scheme merely amplifies these differences and leads to a shift of the ITCZ via the cloud radiative effect.

5. Summary

In this study, the vertical resolution of the General Circulation Model ECHAM has been refined and its effects on the structure of the ITCZ in an aqua-planet setup studied. The chosen configurations have 76, 134, and 192 levels and have been calculated based upon the 47 levels default resolution of ECHAM. This corresponds to a typical grid spacing in the troposphere of 45.6, 22.8, 11.4, and 7.6 hPa for the configurations with 47, 76, 134, and 192 levels, respectively.

The ITCZ location successively shifts equatorward with an increase in vertical resolution. The difference in location between the two extreme configurations amounts to 8.4°. The structure converges to a single ITCZ when using 134 vertical levels.

The primary reason for the sensitivity of the ITCZ structure to the vertical resolution is traced back to a dependency of the mixing formulation of the convection scheme upon the underlying vertical coordinate. The use of a first-order discretization scheme leads to weaker mixing of the updraft's turbulent entrainment/detrainment for a poorly resolved vertical coordinate. Weaker mixing pushes the ITCZ poleward, as found in previous studies. This effect manifests itself by an increase of integrated cloud water content and by the appearance of a secondary maximum in the higher resolution simulations. Turning off the mixing processes in the convection scheme reduces the spread in the ITCZ location among the simulations with a remaining maximum shift of 3.7°. This remaining difference is associated with left-over differences in the relative humidity profiles between the simulations. The low-resolution simulation in particular exhibits larger relative humidity values above 300 hPa and below 900 hPa. These differences affect the location of the ITCZ through their effect on the cloud cover. High-level and low-level cloud amounts increase in the low-resolution simulation. The low-level cloud amount dominates the response and shifts the ITCZ poleward. Turning off entrainment processes and making clouds transparent to radiation remove most of the sensitivity of the ITCZ structure to the vertical resolution, albeit leading to a double ITCZ structure in all simulations.

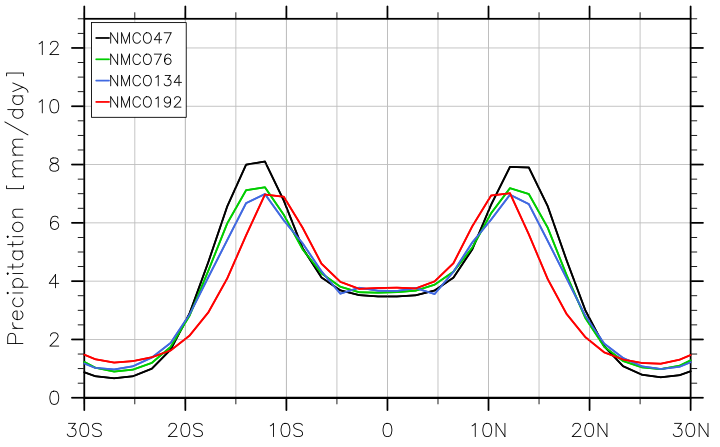

Figure 8. Total precipitation for NMCO47, NMCO76, NMCO134, and NMCO192 experiments without mixing and clouds.

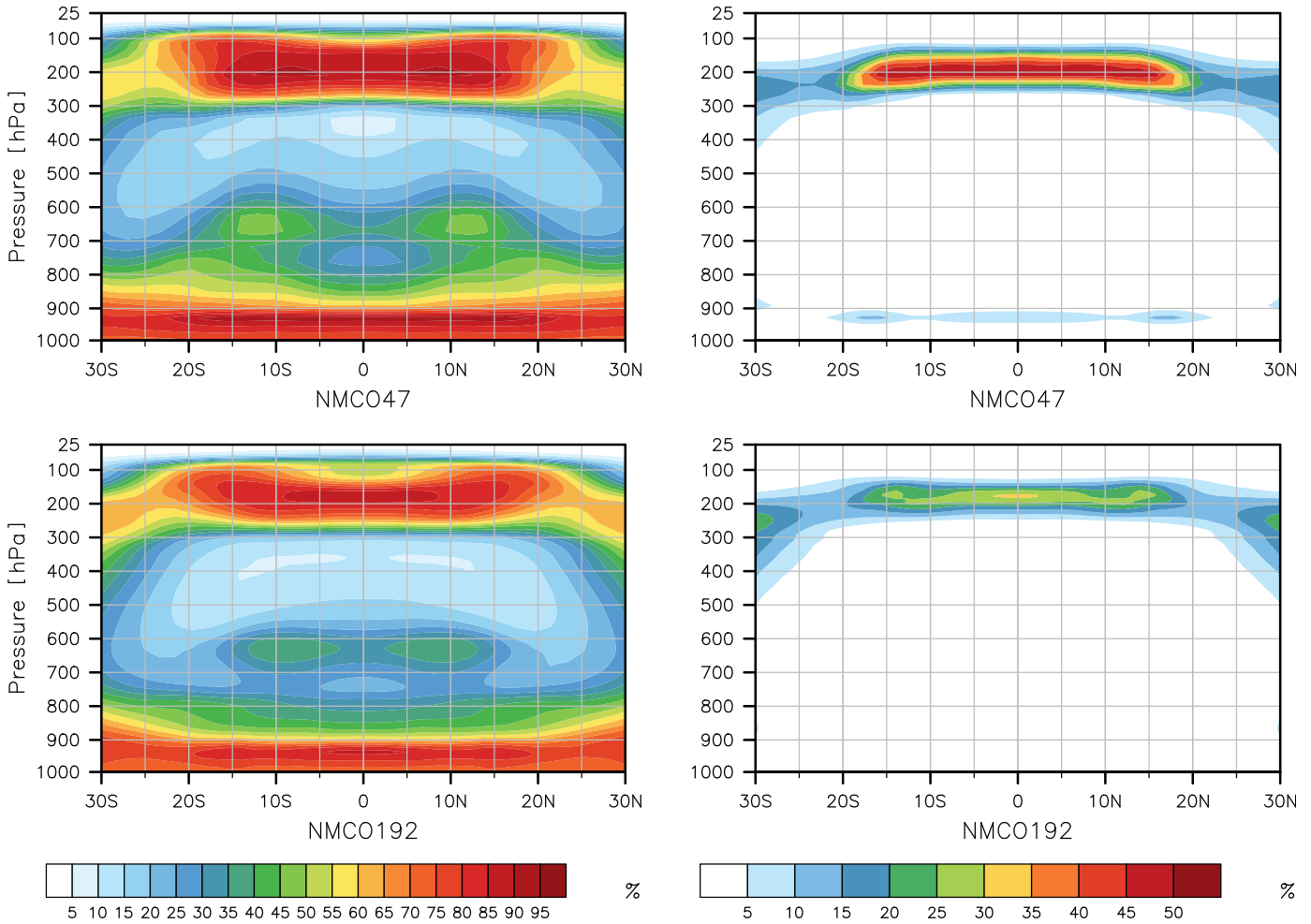

Figure 9. (left) Relative humidity and (right) cloud cover in NMCO47 and NMCO192.

Refining the vertical resolution leads to larger differences in the location of the ITCZ than changing the convection scheme, at least in the General Circulation Model used. As a lot of effort is spent in developing new convective parameterizations and in tuning their implementation toward obtaining one single ITCZ, this suggests that simple tests of numerical consistency, such as done in this study, might need to be more routinely done to ensure that the equations we are solving are the ones we indeed intend to. Likewise correcting for the numerical discretization errors in convective mixing by including second-order terms shifts the ITCZ nearly to the equator.

Acknowledgments

The study was supported by the Max Planck Society for the advancement of science. Use of the supercomputer facilities at the Deutsches Klimarechenzentrum (DKRZ) is acknowledged. Primary data and scripts used in the analysis and other supporting material that may be useful in reproducing the author's work are archived by the Max Planck Institute for Meteorology and can be obtained by contacting publications@mpimet.mpg.de.

References

Bacmeister, J. T., Suarez, M. J., & Robertson, F. R. (2006). Rain reevaporation, boundary layer? Convection interactions and Pacific rainfall patterns in an AGCM. *Journal of the Atmospheric Sciences*, *63*(12), 3383–3403. https://doi.org/10.1175/JAS3791.1

Crueger, T., & Stevens, B. (2015). The effect of atmospheric radiative heating by clouds on the Madden-Julian Oscillation. *Journal of Advances in Modeling Earth Systems*, *7*, 854–864. https://doi.org/10.1002/2015MS000434

Derbyshire, S. H., Beau, I., Bechtold, P., Grandpeix, J.-Y., Piriou, J.-M., Redelsperger, J.-L., & Soares, P. M. M. (2004). Sensitivity of moist convection to environmental humidity. *Quarterly Journal of the Royal Meteorological Society*, *130*(604), 3055–3079. https://doi.org/10.1256/qj.03.130

Harrop, B. E., & Hartmann, D. L. (2016). The role of cloud radiative heating in determining the location of the ITCZ in aquaplanet simulations. *Journal of Climate*, *29*(8), 2741–2763. https://doi.org/10.1175/JCLI-D-15-0521.1

Inness, P. M., Slingo, J. M., Woolnough, S. J., Neale, R. B., & Pope, V. D. (2001). Organisation of tropical convection in a GCM with varying vertical resolution: Implications for the simulation of the Madden-Julian Oscillation. *Climate Dynamics*, *17*(10), 777–793.

Jensen, M. P., & Genio, A. D. D. (2006). Factors limiting convective cloud-top height at the ARM Nauru Island Climate Research Facility. *Journal of Climate*, *19*(10), 2105–2117. https://doi.org/10.1175/JCLI3722.1

Johnson, R. H., Rickenbach, T. M., Rutledge, S. A., Ciesielski, P. E., & Schubert, W. H. (1999). Trimodal characteristics of tropical convection. *Journal of Climate*, *12*(8), 2397–2418. https://doi.org/10.1175/1520-0442(1999)012<2397:TCOTC>2.0.CO;2

Kim, D., Xavier, P., Maloney, E., Wheeler, M., Waliser, D., Sperber, K., . . . Liu, H. (2014). Process-oriented MJO simulation diagnostic: Moisture sensitivity of simulated convection. *Journal of Climate*, *27*(14), 5379–5395. https://doi.org/10.1175/JCLI-D-13-00497.1

Landu, K., Leung, L. R., Hagos, S., Vinoj, V., Rauscher, S. A., Ringler, T., & Taylor, M. (2014). The dependence of ITCZ structure on model resolution and dynamical core in aquaplanet simulations. *Journal of Climate*, *27*(6), 2375–2385. https://doi.org/10.1175/JCLI-D-13-00269.1

Li, G., & Xie, S.-P. (2014). Tropical biases in CMIP5 multimodel ensemble: The excessive equatorial Pacific cold tongue and double ITCZ problems. *Journal of Climate*, *27*(4), 1765–1780. https://doi.org/10.1175/JCLI-D-13-00337.1

Lin, J.-L. (2007). The double-ITCZ problem in IPCC AR4 coupled GCMs: Ocean-atmosphere feedback analysis. *Journal of Climate*, *20*(18), 4497–4525. https://doi.org/10.1175/JCLI4272.1

Mapes, B. E., & Zuidema, P. (1996). Radiative-dynamical consequences of dry tongues in the tropical troposphere. *Journal of the Atmospheric Sciences*, *53*(4), 620–638. https://doi.org/10.1175/1520-0469(1996)053<0620:RDCODT>2.0.CO;2

Mechoso, C., Robertson, A., Barth, N., Davey, M., Delecluse, P., Gent, P., . . . Tribbia, J. (1995). The seasonal cycle over the tropical Pacific in coupled ocean? Atmosphere General Circulation Models. *Monthly Weather Review*, *123*(9), 2825–2838. https://doi.org/10.1175/1520-0493(1995)123<2825:TSCOTT>2.0.CO;2

Medeiros, B., Stevens, B., & Bony, S. (2015). Using aquaplanets to understand the robust responses of comprehensive climate models to forcing. *Climate Dynamics*, *44*(7), 1957–1977. https://doi.org/10.1007/s00382-014-2138-0

Medeiros, B., Stevens, B., Held, I. M., Zhao, M., Williamson, D. L., Olson, J. G., & Bretherton, C. S. (2008). Aquaplanets, climate sensitivity, and low clouds. *Journal of Climate*, *21*(19), 4974–4991. https://doi.org/10.1175/2008JCLI1995.1

Möbis, B. (2013). Factors controlling the position of the inter-tropical convergence zone on an aquaplanet. *Reports on Earth System Science*, *129*(1), 58–62.

Möbis, B., & Stevens, B. (2012). Factors controlling the position of the intertropical convergence zone on an aquaplanet. *Journal of Advances in Modeling Earth Systems*, *4*, M00A04. https://doi.org/10.1029/2012MS000199

Neale, R. B., & Hoskins, B. J. (2000). A standard test for AGCMs including their physical parameterizations: I. The proposal. *Atmospheric Science Letters*, *1*(2), 101–107. https://doi.org/10.1006/asle.2000.0022

Nordeng, T. E. (1994). *Extended versions of the convective parameterization scheme at ECMWF and their impact on the mean transient activity of the model in the tropics* (ECMWF Tech. Memo 206, 41 p). Reading, UK: ECMWF

Oueslati, B., & Bellon, G. (2013). Tropical precipitation regimes and mechanisms of regime transitions: Contrasting two aquaplanet general circulation models. *Climate Dynamics*, *40*(9), 2345–2358. https://doi.org/10.1007/s00382-012-1344-x

Pope, V. D., Pamment, J. A., Jackson, D. R., & Slingo, A. (2001). The representation of water vapor and its dependence on vertical resolution in the Hadley Centre Climate Model. *Journal of Climate*, *14*(14), 3065–3085. https://doi.org/10.1175/1520-0442(2001)014<3065:TROWVA>2.0.CO;2

Randall, D. A., Harshvardhan, D. A., Dazlich, T. G., & Corsetti (1989). Interactions among radiation, convection, and large-scale dynamics in a General Circulation Model. *Journal of the Atmospheric Sciences*, *46*(13), 1943–1970. https://doi.org/10.1175/1520-0469(1989)046<1943:IARCAL>2.0.CO;2

Redelsperger, J.-L., Parsons, D. B., & Guichard, F. (2002). Recovery processes and factors limiting cloud-top height following the arrival of a dry intrusion observed during TOGA COARE. *Journal of Atmospheric Sciences*, *59*, 2438–2457. https://doi.org/10.1175/1520-0469(2002)059<2438:RPAFLC>2.0.CO;2

Roca, R., Lafore, J.-P., Piriou, C., & Redelsperger, J.-L. (2005). Extratropical dry-air intrusions into the West African Monsoon Midtroposphere: An important factor for the convective activity over the Sahel. *Journal of the Atmospheric Sciences*, *62*(2), 390–407. https://doi.org/10.1175/JAS-3366.1

Roeckner, E., Brokopf, R., Esch, M., Giorgetta, M., Hagemann, S., Kornblueh, L., . . . Schulzweida, U. (2006). Sensitivity of simulated climate to horizontal and vertical resolution in the ECHAM5 atmosphere model. *Journal of Climate*, *19*(16), 3771–3791. https://doi.org/10.1175/JCLI3824.1

Slingo, J., Inness, P., Neale, R., Woolnough, S., & Yang, G. (2002). Scale interactions on diurnal to seasonal timescales and their relevance to model systematic errors. *Annals of Geophysics*, *46*(1), 139–155.

Stevens, B., Giorgetta, M., Esch, M., Mauritsen, T., Crueger, T., Rast, S., . . . Roeckner, E. (2013). Atmospheric component of the MPI-M Earth System Model: ECHAM6. *Journal of Advances in Modeling Earth Systems*, *5*, 146–172. https://doi.org/10.1002/jame.20015

Sundqvist, H., Berge, E., & Kristjánsson, J. E. (1989). Condensation and cloud parameterization studies with a mesoscale numerical weather prediction model. *Monthly Weather Review*, *117*(8), 1641–1657. https://doi.org/10.1175/1520-0493(1989)117<1641:CACPSW>2.0.CO;2

Takemi, T., Hirayama, O., & Liu, C. (2004). Factors responsible for the vertical development of tropical oceanic cumulus convection. *Geophysical Research Letters*, *31*, L11109. https://doi.org/10.1029/2004GL020225

Tiedtke, M. (1989). A comprehensive mass flux scheme for cumulus parameterization in large-scale models. *Monthly Weather Review*, *117*(8), 1779–1800. https://doi.org/10.1175/1520-0493(1989)117<1779:ACMFSF>2.0.CO;2

Tompkins, A. M., & Emanuel, K. A. (2000). The vertical resolution sensitivity of simulated equilibrium temperature and water-vapour profiles. *Quarterly Journal of the Royal Meteorological Society*, *126*(565), 1219–1238. https://doi.org/10.1002/qj.49712656502

Williamson, D. L. (2013). Dependence of ape simulations on vertical resolution with the community atmospheric model, version 3. *Journal of the Meteorological Society of Japan. Series II*, *91A*, 231–242. https://doi.org/10.2151/jmsj.2013-A08

Xu, K.-M., & Krueger, S. K. (1991). Evaluation of cloudiness parameterizations using a cumulus ensemble model. *Monthly Weather Review*, *119*(2), 342–367. https://doi.org/10.1175/1520-0493(1991)119<0342:EOCPUA>2.0.CO;2

Zhang, G. J., & Mu, M. (2005). Effects of modifications to the Zhang-McFarlane convection parameterization on the simulation of the tropical precipitation in the National Center for Atmospheric Research Community Climate Model, version 3. *Journal of Geophysical Research*, *110*, D09109. https://doi.org/10.1029/2004JD005617